Field emission and photofluorescent characteristics of zinc oxide nanowires synthesized by a metal catalyzed vapor-liquid-solid process

Seu Yi Li, Pang Lin, Chia Ying Lee, and Tseung Yuen Tseng

Citation: Journal of Applied Physics **95**, 3711 (2004); doi: 10.1063/1.1655685
View online: http://dx.doi.org/10.1063/1.1655685
View Table of Contents: http://scitation.aip.org/content/aip/journal/jap/95/7?ver=pdfcov
Published by the AIP Publishing

Field emission and photofluorescent characteristics of zinc oxide nanowires synthesized by a metal catalyzed vapor-liquid-solid process

Seu Yi Li and Pang Lin
Institute of Materials Science and Engineering, National Chiao Tung University, Hsinchu, Taiwan, 30049, Republic of China

Chia Ying Lee and Tseung Yuen Tseng[a)]
Department of Electronics Engineering and Institute of Electronics, National Chiao Tung University, Hsinchu, Taiwan, 30050, Republic of China

(Received 19 May 2003; accepted 13 January 2004)

The ZnO nanowires synthesized by vapor-liquid-solid growth mechanism with Cu and Au as the catalyst were investigated. The principal differences in morphology between Cu and Au catalyzed ZnO nanowires are observed and lead to significant differences in their field emission and photofluorescent characteristics. The Cu catalyzed ZnO nanowires with a high-quality wurtzite structure were grown vertically on *p*-type Si(100) substrate along [0002] direction. A strong ultraviolet emission at 381 nm is observed. These ZnO nanowires show excellent field emission properties with turn-on field of 0.83 V/μm and corresponding current density of 25 μA/cm^2. The emitted current density of the ZnO nanowires is 1.52 mA/cm^2 at a bias field of 8.5 V/μm. The large field emission area factor, β arising from the morphology of the nanowire field emitter, is partly responsible for the good emission characteristics. The ZnO nanowires with high emission current density and low turn-on field are expected to be used in field emission flat panel display. © *2004 American Institute of Physics.* [DOI: 10.1063/1.1655685]

I. INTRODUCTION

Since carbon nanotubes (CNTs) were discovered in 1991,[1] the worldwide nanotechnology research has been quite extensive on one-dimensional (1D) nanostructures, such as CNTs, oxide nanobelts (or nano ribbons),[2] and nanowires.[3–6] These fascinating structures have drawn much attention because of their interesting growth mechanisms, physical properties, and applications in the electro-optical nanodevices.[7–11] Optical explorations of these nanostructured materials are focused on the field emission and photoluminescence (PL) characteristics. In general, there are three nanowire growth mechanisms: vapor-liquid-solid (VLS) growth mechanism,[12] metalorganic vapor phase epitaxy deposition,[13] and template method.[14] Among these growth mechanisms, the metal catalytic VLS growth mechanism provides a cheap process for large-area deposition of nanowire array. ZnO, a direct band gap (3.37 eV) semiconductor with exciton binding energy of 60 meV, is a suitable material for optical application. Several previous studies have shown that ZnO nanowires exhibit strong UV laser emission, which can be used in luminescent device applications.[15–18] In our study, the ZnO nanowires are synthesized by the VLS process with Cu[19] and Au as the catalysts in Ar atmosphere on *p*-type Si(100) substrate. The morphology, structural, composition, photoluminescence, and field emission characterizations of these nanowires were examined.

[a)]Author to whom correspondence should be addressed; electronic mail: tseng@cc.nctu.edu.tw

II. EXPERIMENT

Before the VLS process, a Radio Corporation of America method was used to clean *p*-type Si(100) substrate and put the substrate in ultrasonic bath of acetone for 30 min. This process can remove the native oxide from the surface of Si substrate. After the cleaning procedure, thin films of Au and Cu were deposited on Si(100) substrate by rf sputtering (13.56 MHz) under 10 mTorr Ar atmosphere using 30 W for 15 s. The thicknesses of Cu and Au thin films were about 70–100 Å. This metal layer acts as a catalyst for ZnO nanowire growth.

The ZnO nanowires were synthesized by VLS process[12] with temperature in the range of 750–950 °C. A quartz boat was filled with a mixture of ZnO and graphite powder and loaded in a horizontal quartz tube furnace with an inner diameter of 7.62 cm. A precisely controlling carrying gas flow pattern (CGFP) method was employed to control the growth process of ZnO nanowires. For such CGFP method, the carrier gas outlet was put into the center of the horizontal furnace and was below the quartz boat about 0.5 cm. The distance between gas outlet and the center of quartz boat was about 75 cm. The rate of increase in temperature was 150 °C/min under high purity Ar (99.998%) atmosphere with the gas flow rate from 20.0 to 100.0 cm^3/s. Besides, we also used general VLS method for the preparation of some Au catalyzed ZnO nanowires for which the gas outlet was located above the quartz boat and other growth conditions were the same as the CGFP method. These two different gas controlled methods were employed to study the effect of synthesis on the structure and property of the ZnO nanowires. In a separate experiment, the Si substrate with metal film was put

in the furnace with the same heating procedures as the VLS process we used. The appearance of such Si substrate surface before VLS growth was observed by atomic force microscopy (AFM, Digital Instrument). The crystal structure of the nanowires was studied by x-ray diffraction (XRD, MAC Science, MXP18, Japan). The morphology of the ZnO nanowires was analyzed by field emission scanning electron microscopy (FE-SEM, Hitachi S-4700I, Japan) and high resolution transmission electron microscopy (HRTEM, Philips tecani-20). The chemical composition of the ZnO nanowires was characterized by Auger electron microprobe (AES, VG Scientific Microlab 350, UK). A photoluminescence analyzer (PL, Hitachi F-4500, Japan) with Xe lamp as an excitation source (320 nm) was used for optical studies at room temperature.

For field emission characteristic, an indium tin oxide glass (16 Ω/□, RiTEK Co., Taiwan) anode was placed at a distance of 320 μm from a tip of ZnO nanowires. A Keithley 237 source-measure unit was used for measuring the current–voltage ($I-V$) and field emission characteristics. Field emission measurements were carried out in a vacuum chamber with a pressure of 1×10^{-5} Torr at room temperature.

III. RESULTS AND DISCUSSION

Figure 1 shows that the surface morphology of Si substrate with Au thin film after heating process is an irregular island structure. However, the surface configuration of Si substrate with Cu thin film is an ordered square or hexagonal island structure. The different surface morphology of catalyst film will affect the distribution of the ZnO nanowires on the Si substrate, which will be described in a later section.

Figure 2 shows the proposed VLS growth mechanism of ZnO nanowires. There are at least four different stages involved in the formation of ZnO nanowires: metal thin film deposition, catalytic nanoparticle formation, nucleation of ZnO and epitaxial growth of ZnO nanowires. In this experiment, the Cu and Au form the nanosized metal droplets.

As the temperature is increased to the reaction temperature, the ZnO was reduced by graphite and $CO_{(g)}$. The corresponding chemical reaction can be expressed as follows:

$$ZnO_{(s)}+C_{(s)}\rightarrow Zn_{(g)}+CO_{(g)}, \tag{1}$$

$$CO_{(g)}+ZnO_{(s)}\rightarrow CO_{2(g)}+Zn_{(g)}. \tag{2}$$

The gaseous products produced by reactions (1) and (2) would adsorb and condense on the catalytic droplets. Subsequently, the following reaction (3) is catalyzed by the metal droplets at solid–liquid interface

$$Zn_{(g)}+CO_{(g)}\rightarrow ZnO_{(s)}+C_{(s)}, \tag{3}$$

$$C_{(s)}+CO_{2(g)}\rightarrow 2CO_{(g)}. \tag{4}$$

As the substrate temperature decreases, the metal droplets form the spherical caps in front of the ZnO nanowires. Sometimes these droplets will be burnt away for the longer time VLS process. The substrate surface indicated a light or dark gray color after reaction.

The SEM photographs [Figs. 3(a) and 3(b)] show the microstructure of the ZnO nanowires synthesized with Au and Cu by CGFP method. Figure 3(a) illustrates the morphology of the ZnO nanowires grown with Au as the catalyst. Randomly distributed hexagonal pillars exist on the Si substrate. The lengths of these nanowires are ~5 μm and diameters are in the range from 20 to 30 nm. The morphology of the nanowires synthesized with Cu as the catalyst is shown in Fig. 3(b). The ZnO nanowires are well aligned on the Si substrate with a length of 5 μm and diameter of 50 nm. But the morphology of Cu catalyzed ZnO nanowires is quite different from that of Au catalyzed nanowires. This is due to the different liquefaction temperature of the catalytic metal. As the temperature rises in the VLS process, Au–Si alloy droplet formed rapidly on the Si substrate because of the low eutectic point (360 °C)[20] of the Au–Si alloy. Therefore, the surface of the Au film is the larger irregular island structure and the orientation of Si substrate affects the growth direction of the ZnO nanowires. When the Cu is employed in the VLS process, Cu–Si alloy droplets are hard to

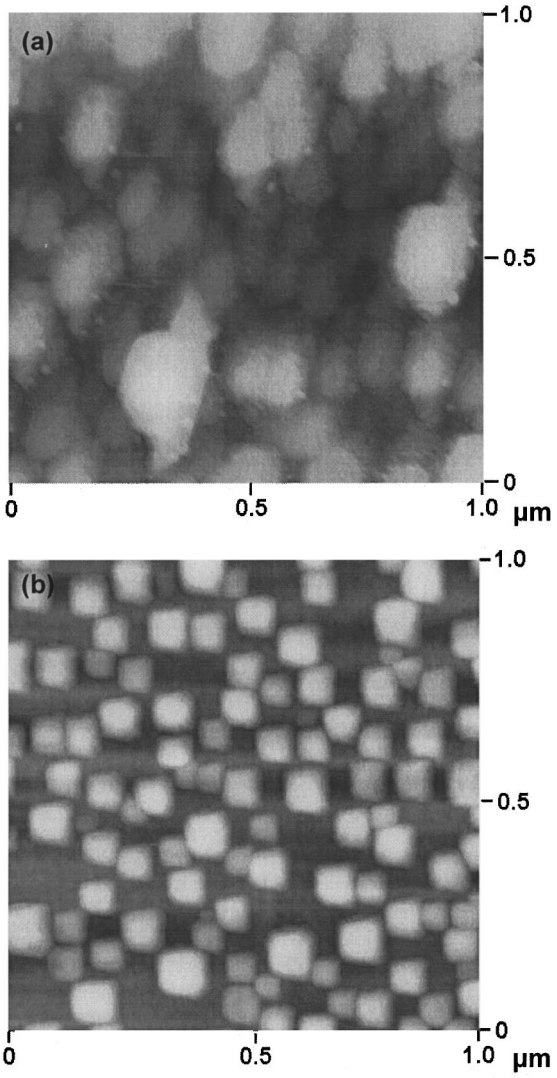

FIG. 1. AFM images of the (a) Au and (b) Cu thin film surface after heating process.

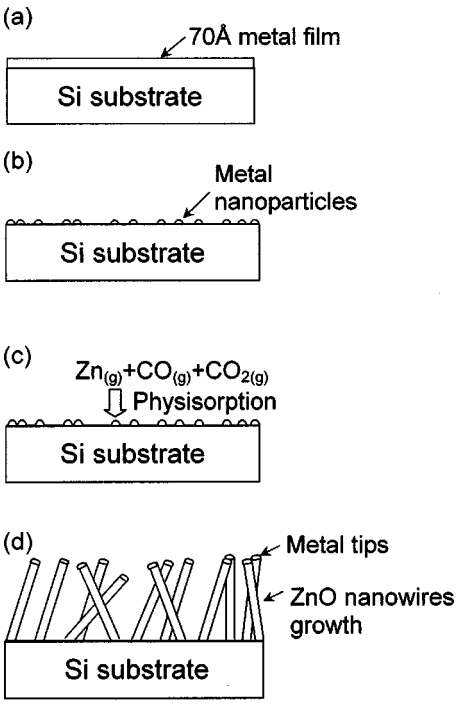

FIG. 2. Schematic illustration of VLS nanowire growth mechanism (a) metal film deposition, (b) metal nanoparticles formation, (c) absorption and nucleation, (d) epitaxial growth.

form on the surface for the high eutectic point (802 °C)[20] of Cu–Si alloy. The surface of the Cu catalyst film has many ordered square and hexagonal Cu island structures and the lattice parameter of Cu ($a=3.215$ Å) is close to that of the ZnO ($a=3.253$ Å). Consequently, the ZnO nanowires can vertically grow from Cu layer on the Si substrate with CGFP method.

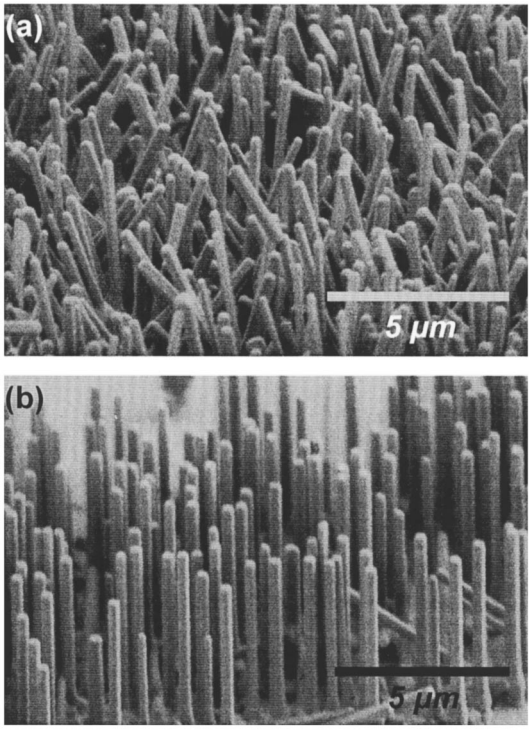

FIG. 3. FE-SEM photographs for (a) Au and (b) Cu catalyzed ZnO nanowires synthesized on *p*-type Si(100) substrate with adopting CGFP method.

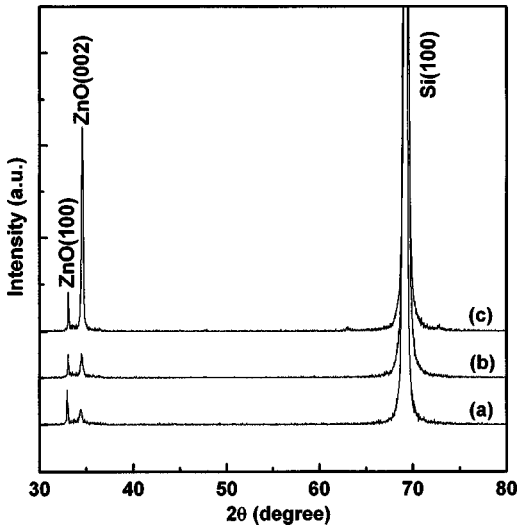

FIG. 4. XRD patterns of ZnO nanowires synthesized with (a) Au as the catalyst, (b) Au as the catalyst by CGFP method, and (c) Cu as the catalyst by CGFP method.

The XRD patterns of ZnO nanowires synthesized with Au and Cu as the catalysts are shown in Fig. 4. As seen in the Fig. 4(a), there exist weak diffraction peaks identified as (100) and (002) of the ZnO nanowires synthesized with Au as the catalyst, which is attributed to the random and disordered distribution of the ZnO nanowires dispersed on the Si substrate [Fig. 3(a)]. When the CGFP method was adopted, the ZnO nanowires had higher (002) peak intensity. Furthermore, the ZnO nanowires also have excellent preferred (002) orientation of Fig. 4(c) when replacing the catalyst from Au to Cu by the CGFP method. The appearance of well crystallized and vertically directed nanowires was also demonstrated on a SEM photograph in Fig. 3(b).

The HRTEM image of Cu-catalyst nanowires shown in Fig. 5 indicates the lattice fringes along [0002] direction of the ZnO nanowires. The spacing of the lattice fringes along the *c* axis of the ZnO nanowire is ~5.21 Å, which is identi-

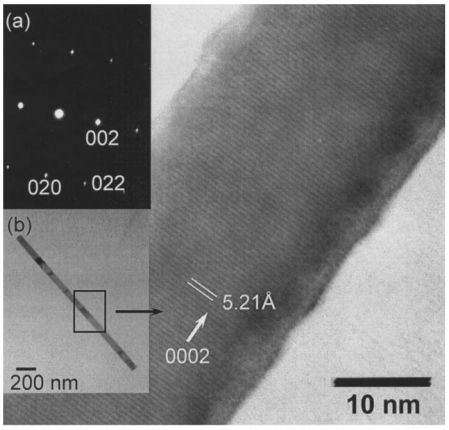

FIG. 5. HRTEM image of Cu catalyzed ZnO nanowires. The selected area electron diffraction (SAED) pattern is shown in inset (a), while bright view image for sidewall of the ZnO nanowires, is indicated in inset (b).

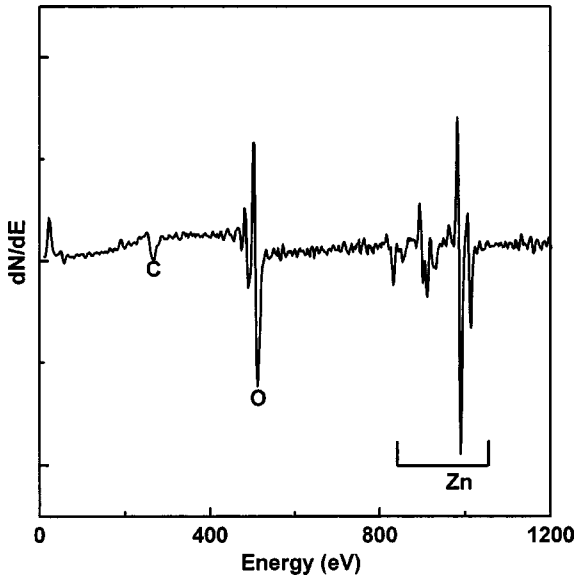

FIG. 6. Typical AES spectrum of Cu catalyzed ZnO nanowires.

cal to the recorded pattern in International Centre for Diffraction Data–Joint Committee on Powder Diffraction Standards No. 80-0075 of ZnO bulk material. The selected area electron diffraction (SAED) pattern is shown in the inset of Fig. 5(a). The direct beam is along (200), and the diffraction pattern of the ZnO nanowire reveals that this nanostructure is single crystalline. After diffraction pattern analysis, the indexed zone axis (002), (020), (022) can be labeled. The result demonstrated that the Cu catalyst-assisted fabrication of ZnO nanowires leads to perfect wurtzite (hcp) crystalline structure. In Fig. 5(b), the bright view image showed the smooth sharp sidewall of the ZnO nanowires, which also proved the CGFP method is helpful in controlling the morphology of the ZnO nanowires.

Figure 6 depicts the AES spectrum of the ZnO nanowires, indicating that the chemical compositions of the ZnO nanowires have two major elements, Zn and O, and one minor contaminant, C. Three strong intense signals of Zn are located at 833, 913, and 991 eV; two signals of O are located at 488 and 510 eV. The weak C signal peak at 273 eV is derived from the carbothermal route adopted for the synthesis of the ZnO nanowires. After noise calibration and integrated calculation, the Zn and O atomic ratio is around 1:1 which is identical with transmission electron microscopy-energy dispersive spectroscopy analysis result.

Figure 7(a) depicts the photoluminescence (PL) spectra at room temperature of the ZnO nanowires which were synthesized with Cu, and Au as catalysts by the CGFP method, and with Au as the catalyst without the CGFP method, respectively. According to the figure, a strong UV emission (~381 nm) and weak green emission (~501–570 nm) are observed in the PL spectrum of the ZnO nanowires synthesized with Cu as the catalyst under the control of CGFP method. The strong UV emission (~381 nm) is due to the near band edge emission of the wide band gap of ZnO, while the weak intensity of green emission (~501–570 nm) is ascribed to the singly ionized oxygen vacancies in ZnO.[21] Therefore, we can suggest that there should be a few oxygen

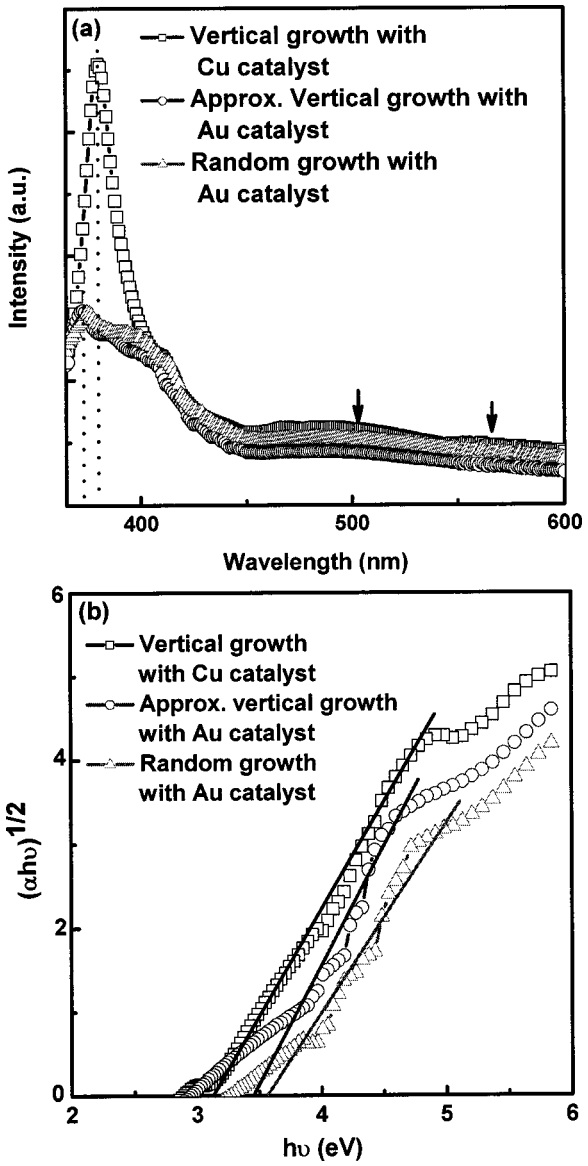

FIG. 7. (a) PL spectra of the ZnO nanowires grown on the *p*-type Si substrate. (b) Tauc's plot of the ZnO nanowires grown on the *p*-type Si substrate.

vacancies in these ZnO nanowires that are synthesized with Cu as the catalyst under the control of the CGFP method. It is easy to perceive the contrast between the PL spectra of ZnO nanowires synthesized with Cu and Au as the catalysts. That is, a little wavelength shift, from 381 to 368 nm, exists in the spectra of the shorter length (3 μm) and randomly distributed nanowires synthesized with Au as the catalyst. This is because of the rare catalyst materials, such as Cu and Au, which diffuse in the ZnO nanowires and serve as the recombination centers. In order to realize the relationship between the impurities and the optical characteristics, the absorption coefficient measurement was taken, and the optical band gap of the ZnO nanowires was calculated by Tauc's[22] plot [Fig. 7(b)]. By the Tauc[22] equation, the optical band gap (E_g) can be determined from the intercept of $(\alpha h\nu)^{1/2}$ vs $h\nu$ plot, where α is the absorption coefficient, h is the Planck constant, and ν is the frequency of radiation. As shown in Fig. 7(b), the Tauc plot provides an estimate of the optical band gaps of these ZnO nanowires. Of those, the ZnO

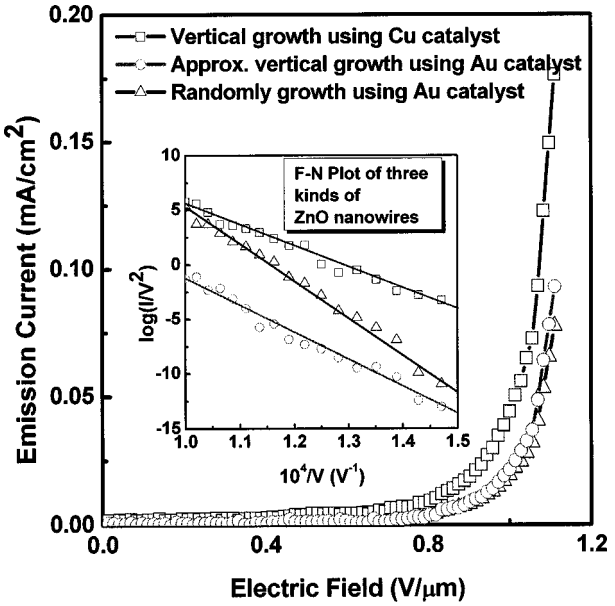

FIG. 8. Field emission characteristics of the ZnO nanowires grown on *p*-type Si substrates. The inset reveals the FN plots of the ZnO nanowires.

nanowires, which were synthesized with Cu as the catalyst by the CGFP method, have the smallest optical band gap with 3.24 eV. The Au catalyzed ZnO nanowires without adopting the CGFP method have a 3.45 eV optical band gap. The largest optical band gap is obtained for the ZnO nanowires synthesized with Au as the catalyst by the CGFP method, having 3.52 eV. It is known that the shorter optical band gap is responsible for the longer emitted wavelength. On the other hand, the impurities which incorporate in the ZnO nanowires cause the various optical band gaps and the UV band emission properties. In addition, the randomly distributed ZnO nanowires synthesized with Au as the catalyst without using the CGFP method have the weak UV emission intensity. It implies that the disordered distribution of the ZnO nanowires decreases the UV emission ability of the ZnO nanowires.

Figure 8 displays the field emission $I-V$ plots for the well-aligned and randomly grown ZnO nanowire array using different metal catalysts. The $I-V$ characteristics of ZnO nanowires grown with different metal catalysts (Fig. 3) followed a Fowler–Nordheim (FN)[23–25] behavior, which is shown in the inset of Fig. 8 where $\ln(I^2/V)$ is plotted as a function of $10^4/V$ (FN plot) and characterized by three constant slopes of FN plots of Cu and Au catalyzed nanowires using the CGFP method and Au catalyzed nanowires without adopting the CGFP method, respectively. When the work function of the nanowires is known, the field emission area factor β can be obtained from the slope of FN plot. The work function for the ZnO nanowire has been reported to be 5.37 eV.[23–25] The β value of Cu catalyzed ZnO nanowires is about 7.18×10^3. The other β values of Au catalyzed with and without adopting the CGFP method are 4.70×10^3 and 3.81×10^3, respectively. The β value of the Cu catalyzed ZnO nanowires is the bigger than those catalyzed by Au, that is, the Cu catalyzed ZnO nanowires display much larger efficient emission area than Au catalyzed nanowires. The field emission area factor β usually depends on the geometry, structure, tip size and number densities of the ZnO nanowires grown on the substrate. Our Cu catalyzed ZnO nanowires exhibit higher β value (that is, larger field emission efficiency) than other reported ZnO nanowires[26] ($\beta=847$) and CNTs[27] ($\beta=1.1\times10^3$) mainly because of their vertical growth, better crystalline structure (Fig. 4) and lower density (Fig. 3). On the other hand, the field-adjustment factor α, which is an index, determined the ability to enhance local field from the field emission tips. In our experiment, α values are 1.21×10^{-5}, 0.92×10^{-5} and 0.88×10^{-5} for Cu catalyzed ZnO nanowires and Au catalyzed ZnO nanowires with and without adopting the CGFP method, respectively. This result indicates that α value for Cu catalyzed ZnO nanowires is larger than those of Au catalyzed ZnO nanowires, which means that vertical growth tips of the ZnO nanowires have better ability to enhance local field.

On the basis of Fig. 8, the turn-on field of Cu catalyzed ZnO nanowires is 0.82 V/μm at current density of 25.0 μA/cm^2. The emission current density is 1.5 mA/cm^2 at an applied field of 8.5 V/μm. The turn-on fields and corresponding current densities for Au catalyzed ZnO nanowires with and without adopting the CGFP method are 0.92 V/μm, 13.0 μA/cm^2 and 0.97 V/μm, 12.7 μA/cm^2, respectively. Our Cu catalyzed ZnO nanowires exhibit lower turn-on voltage and higher emission current densities than the ZnO nanowires synthesized by Lee's research group,[26] which were about 6.0 V/μm and emission current density of 1.0 mA/cm^2 at a bias field of 11.0 V/μm, respectively. These results illustrate that the ZnO nanowire array is sufficient for flat panel field emission display applications in the future.

IV. CONCLUSIONS

In summary, well-aligned and vertically grown Cu catalyzed ZnO nanowires, which have an excellent wurtzite structure, less contamination and precise chemical composition, were successfully grown at 750–950 °C by adopting a CGFP method. The ZnO nanowires emitted strong UV at ~381 nm at room temperature by using Xe lamp (320 nm) as the excitation source. The field emission measurements indicated high emission current density of 1.5 mA/cm^2 under the field of 8.5 V/μm and low turn-on field of 0.83 V/μm at current density of 25 μA/cm. The Cu catalyzed ZnO nanowires exhibited a higher field emission area factor of about 7.18×10^3 and a larger field adjustment factor of 1.21×10^{-5} than those values of Au catalyzed nanowires, which is due to the vertical direction growth of Cu catalyzed nanowires. Such a vertically grown ZnO nanowire array is a good candidate for the future flat panel display applications.

ACKNOWLEDGMENT

This work was supported by the National Science Council of ROC under Contract No. NSC 92-2216-E009-022.

[1] S. Iijima, Nature (London) **354**, 56 (1991).
[2] J. Zhang and L. Zhang, Chem. Phys. Lett. **363**, 293 (2002).
[3] C. Wang, M. Chen, G. Zhu, and Z. Lin, J. Colloid Interface Sci. **243**, 362 (2001).
[4] A. Fert and L. Piraux, J. Magn. Magn. Mater. **200**, 358 (1999).

[5] C. C. Tang, S. S. Fan, M. Lamy de la Chapelle, and P. Li, Chem. Phys. Lett. **333**, 12 (2001).
[6] N. Wang, Y. F. Zhang, Y. H. Tang, C. S. Lee, and S. T. Lee, Phys. Rev. B **58**, 16024 (1998).
[7] D. M. Bagnall, Y. F. Chen, Z. Zhu, T. Yao, S. Koyama, M. Y. Shen, and T. Goto, Appl. Phys. Lett. **70**, 2230 (1997).
[8] M. T. Björk, B. J. Ohlsson, T. Sass, A. I. Persson, C. Thelander, M. H. Magnusson, K. Deppert, L. R. Wallenberg, and L. Samuelson, Appl. Phys. Lett. **80**, 1058 (2002).
[9] M. H. Huang, S. Mao, H. Feick, H. Yan, Y. Wu, H. Kind, E. Weber, R. Russo, and P. Yang, Science **292**, 1897 (2001).
[10] Y. S. Lee and T. Y. Tseng, J. Mater. Sci. Materi. Electron. **9**, 65 (1998).
[11] Y. W. Wang, L. D. Zhang, G. Z. Wang, X. S. Peng, Z. Q. Chu, and C. H. Liang, J. Cryst. Growth **234**, 171 (2002).
[12] M. Huang, S. Mao, H. Feick, H. Yan, Y. Wu, H. Kind, E. Weber, R. Russo, and P. Yang, Science **292**, 2242 (2001).
[13] Y. Wu, R. Fan, and P. Yang, Int. J. Nanosci. **1**, 1 (2002).
[14] Y. Li, G. W. Meng, L. D. Zhang, and F. Phillip, Appl. Phys. Lett. **76**, 2011 (2000).
[15] J. S. Leea, M. I. Kanga, S. Kima, M. S. Leeb, and Y. K. Lee, J. Cryst. Growth **249**, 201 (2003).
[16] K. Park, J. S. Lee, M. Y. Sung, and S. Kim, Jpn. J. Appl. Phys., Part 1 **41**, 7317 (2002).
[17] Y. K. Tseng, I. N. Lin, K. S. Liu, T. S. Lin, and I. C. Chen, J. Mater. Res. **18**, 714 (2003).
[18] H. T. Ng, B. Chen, J. Li, J. Han, M. Meyappan, J. Wu, S. X. Li, and E. E. Haller, Appl. Phys. Lett. **82**, 2023 (2003).
[19] S. Y. Li, C. Y. Lee, and T. Y. Tseng, J. Cryst. Growth **247**, 357 (2003).
[20] H. Baker, H. Okamoto, S. D. Henry, G. M. Davidson, M. A. Fleming, L. Kacprzak, and H. F. Lampman, *ASM Handbook* (ASM International, Ohio, 1987), Vol. 3, pp. 2–76.
[21] K. Vanheusden, W. L. Warren, C. H. Seager, D. R. Tallant, J. A. Voigt, and B. E. Gnade, J. Appl. Phys. **79**, 7983 (1996).
[22] J. Tauc, *Optical Properties of Solids*, edited by F. Abeles (North-Holland, Amsterdam, 1972).
[23] S. H. Yang and M. Yokoyama, Mater. Chem. Phys. **51**, 1 (1997).
[24] L. Nilsson, O. Groening, C. Emmenegger, O. Kuettel, E. Schaller, L. Schlapbach, H. Kind, J.-M. Bonard, and K. Kern, Appl. Phys. Lett. **76**, 2071 (2000).
[25] W. Que, Y. Zhou, Y. L. Lam, Y. C. Chan, C. H. Kam, B. Liu, L. M. Gan, C. H. Chew, G. Q. Xu, S. J. Chua, S. J. Xu, and F. V. C. Mendis, Appl. Phys. Lett. **73**, 2727 (1998).
[26] C. J. Lee, J. J. Lee, S. C. Lyu, Y. Zhang, H. Ruh, and H. J. Lee, Appl. Phys. Lett. **81**, 3648 (2002).
[27] I. Alexandrou, E. Kymakis, and G. A. J. Amaratunga, Appl. Phys. Lett. **80**, 1435 (2002).